International Journal of Scientific & Engineering Research, Volume 5, Issue 5, May-2014
ISSN 2229-5518

Modeling of Fiber Microbuckling in Composite Materials

Takeaki Nadabe, Nobuo Takeda

Abstract— In this study, a model of fiber microbuckling in composite materials is proposed for the purpose of material strength analysis. Firstly the fiber microbuckling is numerically simulated using finite element method in order to understand how this deformation phenomenon appears in the material. Then the equations expressing deformation of composite materials are compiled, and the correspondence between the equations and the actual deformation phenomenon in composite materials are considered. It is indicated that onset of arbitrariness in solution of equations expressing the deformation of composite materials is closely related with the initiation of the fiber microbuckling in composite materials and thus the material strength of composite materials.

Index Terms— Fiber microbuckling, material strength, nonlinear deformation, composite materials

1 Introduction

COMPOSITE materials commonly have complex internal structures including fibers, matrix, interfaces and interlaminar regions, and when precise evaluation of fracture strength of the material is conducted, the internal fracture process in the materials is necessary to be taken into account in the numerical analysis [1]. In recent years, composite materials are being increasingly used in several industrial fields, and the precise evaluation of mechanical response of the material under various loading condition and environmental condition increases the necessity in design and improvement of industrial products [2]. Compressive failure is one of the typical failure modes in fiber reinforced composite materials [3], and fracture strength in compressive failure often becomes one of the limiting factors at the design phase of structural elements [4]. Not only uniaxial compressive strength but also compressive strength at around open holes and post-impact compressive strength in the materials are related to the fundamental compressive strength of the materials, and improvement of compressive strength would be related with the increase of the light weight potential of the materials. In this study, a model of fiber microbuckling in composite materials is proposed. Firstly the fiber microbuckling is numerically simulated using finite element method to understand how this deformation phenomenon appears in the material, and then the model of this phenomenon is considered.

2 Numerical Simulation of Fiber Microbuckling

2.1 Numerical Model

In order to investigate the physical mechanism of fiber microbuckling in composite materials, the numerical simulation of fiber microbuckling is conducted. Finite element method is used to simulate the fiber microbuckling. Fig. 1 shows the numerical model of this analysis. The white and gray elements in Fig. 1 represent fibers and matrix, respectively. The thickness of the ply in y-direction is 0.60 mm. The length in x-direction is 1.0 mm, and the thickness in z-direction is 100 mm. The diameter of each fiber is set to 3.5 μm, and the interval of fibers is 20.0 μm. The fiber volume fraction of the materials is set to 17.5 %. Each fiber and matrix is modeled by two-dimensional plate elements. The one fiber placed at the center has the initial misalignment as shown in the figure. The initial misalignment of the fiber is introduced using the sine function. The x coordinate of each node is placed regularly at the interval of 5.0 μm, and the y coordinate of each node is calculated using the sine function. The other fibers are modeled as the straight lines and the fiber axial direction is parallel to the x-direction.

Due to the atomic structure in the inside of the fibers, the fibers commonly have the different material property in between fiber axial and transverse directions. Here, the fibers are modeled by the transversely isotropic elastic material. Table 1 shows the material property of the fibers. Carbon fiber AS4 (Hexcel Corp.) is assumed [5]. Matrix is modeled by isotropic elastic-plastic material. Commonly the compressive failure of composite materials is affected by the nonlinear stress-strain relation of matrix, thus in this analysis the nonlinear stress-strain curve of matrix shown in Fig. 2 (hardening curve N) is applied, and the nonlinear finite element analysis is conducted. Table 2 shows the material property of matrix. Epoxy resin 3501-6 (Hercules Chemical Company, Inc.) is assumed [5]. The quasi-static and room temperature environment are assumed in the analysis.

- *Takeaki Nadabe E-mail: nadabe@smart.k.u-tokyo.ac.jp*
- *Nobuo Takeda E-mail: takeda@smart.k.u-tokyo.ac.jp*

Since the geometrical nonlinearity commonly affects the buckling phenomena of the materials, the geometrical nonlinear effect is incorporated in the analysis. The incremental analysis in the finite element analysis is conducted by the arc-length method. In the initial increment, the average applied strain to the material in x-direction is set to 0.002 %. The analysis is conducted until the average applied strain 2.0 %. The domain decomposition method is applied to conduct the parallel computing in the numerical calculation. The authors produced fortran program for this analysis, and the analysis is conducted using this program.

2.2 Simulated Results and Discussions

Fig. 3 and 4 show the simulated results of deformation and stress distribution of the material, respectively. Simulated results show that in the initial state of the loading, the stress concentration occurs in the material around the initial misalignment of fiber, and when the applied load is increased, local areas of matrix around the stress concentration start to yield, and deformation is locally increased. At one moment of the loading, a large deformation occurs within a narrow band, and a band of localized deformation develops rapidly. This band of localized deformation passes across the misalignment part of center fiber. As shown in the figures, fibers cause bending deformation, and fiber direction is largely rotated. Matrix causes shear deformation, and the shape of the elements is close to rhombus shape which is rectangle shape in initial state. After the yielding of matrix, the elastic-plastic tangent shear stiffness of matrix significantly reduces, and the shear strain rapidly increases. Then the shear

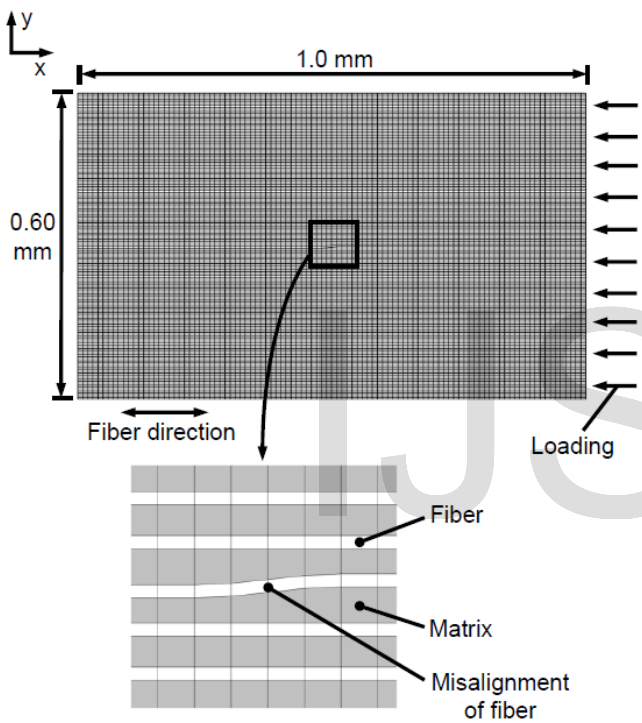

Fig. 1. Numerical model of composite material.

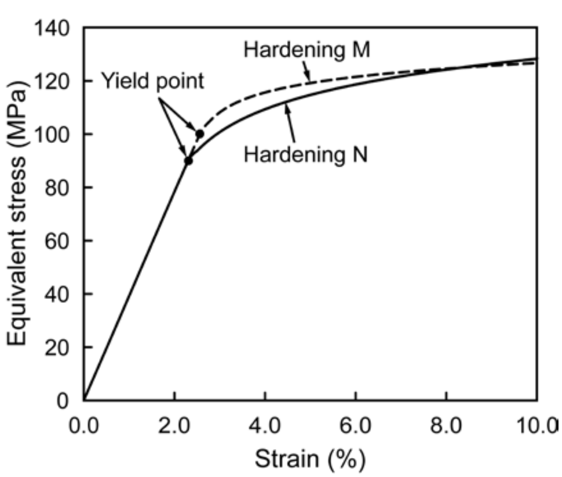

Fig. 2. Stress-strain curve of matrix.

TABLE 1
MATERIAL PROPERTY OF FIBER [5]

Elastic modulus in fiber axial direction	225	GPa
Elastic modulus in transverse direction	15	GPa
In-plane Poisson's ratio	0.2	
In-plane shear modulus	15	GPa
Transverse shear modulus	7	GPa

TABLE 2
MATERIAL PROPERTY OF MATRIX [5]

Elastic modulus	4.2	GPa
Poisson's ratio	0.34	
Yield stress	90	MPa

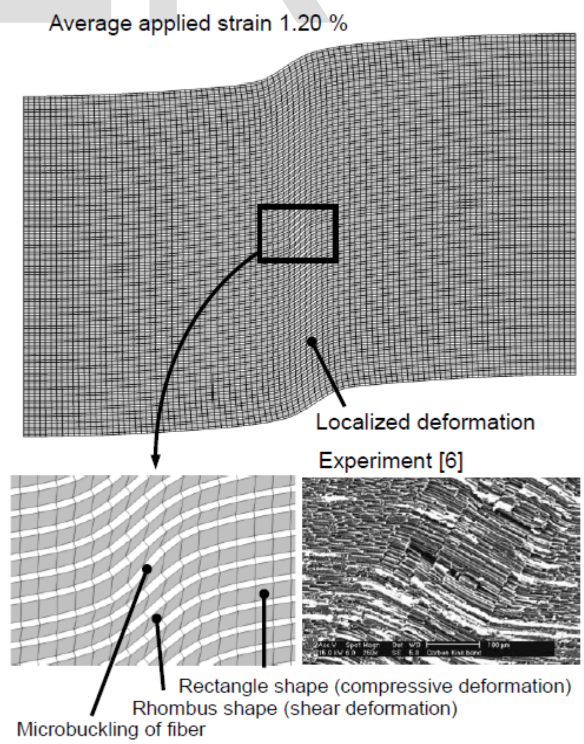

Fig. 3 Simulated results of deformation.

ISSN 2229-5518

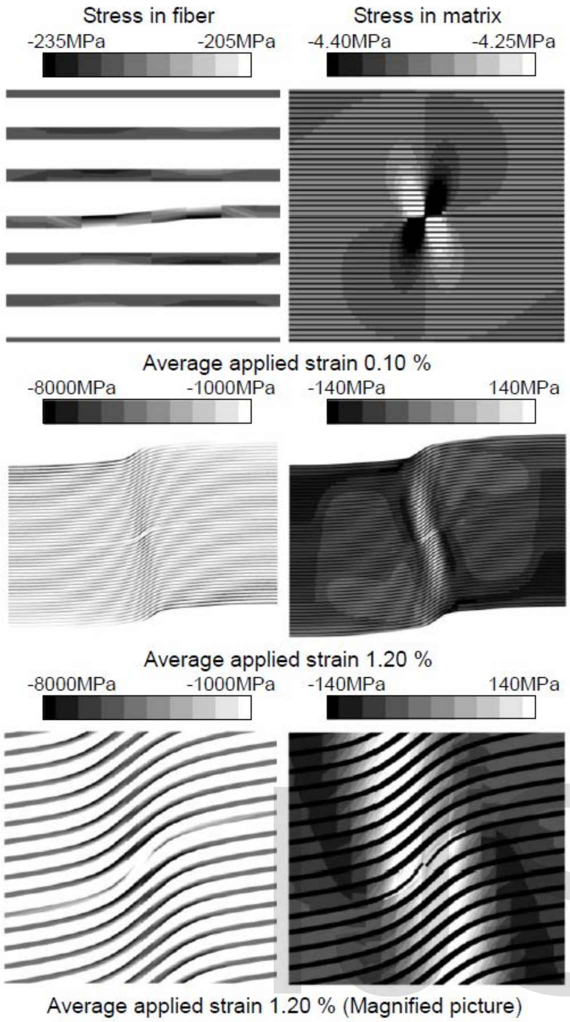

Fig. 4 Simulated results of stress distribution.

deformation of this part of matrix increases, and due to the shear deformation of the part, the band of localized deformation is formed. The reduction of tangent shear stiffness of matrix after yielding is the essential factor in the onset of the microbuckling of the fibers.

3 Modeling of Fiber Microbuckling

3.1 Equations Expressing Deformation of Composite Materials

Here, the equations expressing deformation of composite materials are compiled. The equations consist of motion equation and constitutive equation. The motion equation is represented as the following,

$$\rho_0 \frac{\partial^2 u_i}{\partial t^2} = \frac{\partial P_{ij}}{\partial X_j} + \rho_0 f_i \tag{1}$$

where ρ_0 is density, t is time, u_i is displacement, X_j is coordinate at reference configuration, P_{ij} is the first Piola-Kirchhoff stress and f_i is external force. The nonlinear stress-strain relation of composite materials is represented by the nonlinear deformation theory shown by Tohgo et al. [7].

$$d\boldsymbol{\sigma} = \boldsymbol{C}_{comp} d\boldsymbol{\varepsilon}$$

$$\boldsymbol{C}_{comp} = \boldsymbol{C}_m \left\{(1 - V_f)(\boldsymbol{C}_f - \boldsymbol{C}_m)\boldsymbol{S} + \boldsymbol{C}_m\right\}^{-1} \boldsymbol{K} \tag{2}$$
$$\boldsymbol{K} = (1 - V_f)\left\{(\boldsymbol{C}_f - \boldsymbol{C}_m)\boldsymbol{S} + \boldsymbol{C}_m\right\} + V_f \boldsymbol{C}_f$$

where $d\boldsymbol{\sigma}$ is stress rate, $d\boldsymbol{\varepsilon}$ is strain rate, $\boldsymbol{C}_{comp}$, $\boldsymbol{C}_f$ and $\boldsymbol{C}_m$ are constitutive tensors of composites, fibers and matrix, respectively, V_f is fiber volume fraction and $\boldsymbol{S}$ is Eshelby tensor. Next, the effect of geometrical nonlinearity during the material deformation is considered. Here the constitutive tensor in spacial description is defined in the relation between the second Piola-Kirchhoff stress and the right Cauchy-Green deformation tensor.

$$C^{spa}_{abcd} = \frac{\partial S_{ab}}{\partial C^{CG}_{cd}} \tag{3}$$

where C^{spa}_{abcd} is constitutive tensor in spacial description, S_{ab} is the second Piola-Kirchhoff stress and C^{CG}_{cd} is the right Cauchy-Green deformation tensor. The constitutive tensor in material description is represented by the constitutive tensor in spacial description as follows,

$$\begin{aligned} C^{mat}_{ijkl} &= 2J^{-1} F_{ia} F_{jb} F_{kc} F_{ld} C^{spa}_{abcd} \\ &= 2\frac{1}{J}\frac{\partial x_i}{\partial X_a}\frac{\partial x_j}{\partial X_b}\frac{\partial x_k}{\partial X_c}\frac{\partial x_l}{\partial X_d} C^{spa}_{abcd} \end{aligned} \tag{4}$$

where C^{mat}_{ijkl} is constitutive tensor in material description, F_{ia} is deformation gradient, $J = \det F_{ij}$ is Jacobian and x_i is coordinate at present configuration. Cauchy stress is represented by the second Piola-Kirchhoff stress, deformation gradient and Jacobian as follows,

$$\sigma_{ij} = J^{-1} F_{ik} S_{kl} F_{jl} \tag{5}$$

$$\begin{aligned} \dot{\sigma}_{ij} &= J^{-1} \dot{F}_{ik} S_{kl} F_{jl} + J^{-1} F_{ik} \dot{S}_{kl} F_{jl} \\ &\quad + J^{-1} F_{ik} S_{kl} \dot{F}_{jl} - \dot{J} J^{-1} F_{ik} S_{kl} F_{jl} \end{aligned} \tag{6}$$

where σ_{ij} is Cauchy stress and $\dot{\sigma}_{ij}$ is the material time derivative of Cauchy stress. Here, the time derivative of deformation gradient and Jacobian is

$$\dot{F}_{ij} = L_{ik} F_{kj}, \quad \dot{J} = L_{ii} \tag{7}$$

where L_{ik} is velocity gradient. Then

$$\begin{aligned} \dot{\sigma}_{ij} &= J^{-1} L_{im} F_{mk} S_{kl} F_{jl} + J^{-1} F_{ik} \dot{S}_{kl} F_{jl} \\ &\quad + J^{-1} F_{ik} S_{kl} F_{ml} L_{jm} - J^{-1} L_{mm} F_{ik} S_{kl} F_{jl} \\ &= J^{-1} F_{ik} \dot{S}_{kl} F_{jl} + L_{ik}\sigma_{kj} + \sigma_{ik} L_{jk} - \sigma_{ij} L_{ll} \end{aligned} \tag{8}$$

where

$$\begin{aligned} \dot{S}_{kl} &= C^{spa}_{klmn} \cdot \dot{C}^{CG}_{mn} = C^{spa}_{klmn} \dot{F}_{om} F_{on} + C^{spa}_{klmn} F_{om} \dot{F}_{on} \\ &= C^{spa}_{klmn} L_{op} F_{pm} F_{on} + C^{spa}_{klmn} F_{om} L_{op} F_{pn} \end{aligned} \tag{9}$$

$$\begin{aligned} J^{-1} F_{ik} \dot{S}_{kl} F_{jl} &= J^{-1} F_{ik} F_{jl} F_{pm} F_{on} C^{spa}_{klmn} L_{op} \\ &\quad + J^{-1} F_{ik} F_{jl} F_{om} F_{pn} C^{spa}_{klmn} L_{op} \\ &= \frac{1}{2} C^{mat}_{ijpo} L_{op} + \frac{1}{2} C^{mat}_{ijop} L_{op} \\ &= C^{mat}_{ijkl} \cdot \frac{1}{2}(L_{lk} + L_{kl}) = C^{mat}_{ijkl} D_{kl} \end{aligned} \tag{10}$$

Therefore

$$\dot{\sigma}_{ij} = C^{mat}_{ijkl} D_{kl} + L_{ik}\sigma_{kj} + \sigma_{ik} L_{jk} - \sigma_{ij} L_{ll} \tag{11}$$

This coinsides with the formulation of Truesdell rate of Cauchy stress. There, here the formulation of finite deformation is based on Truesdell rate of Cauchy stress. Then the rate of the first Piola-Kirchhoff stress is represented as follows,

$$\dot{P}_{ij} = J\frac{\partial X_j}{\partial x_k}\left(\dot{\sigma}_{ik} + \sigma_{ik}L_{ll} - \sigma_{il}L_{kl}\right)$$
$$= J\frac{\partial X_j}{\partial x_m}\left(C^{mat}_{imkl}D_{kl} + \sigma_{lm}L_{il}\right)$$
$$= J\frac{\partial X_j}{\partial x_m}\left(C^{mat}_{imkl} + \sigma_{lm}\delta_{ik}\right)\frac{\partial \dot{u}_k}{\partial x_l} \qquad (12)$$

where δ_{ik} is Kronecker delta. From (1) and (12), a set of equations expressing deformation of composite materials is obtained.

$$\rho_0\frac{\partial^2 u_i}{\partial t^2} = \frac{\partial P_{ij}}{\partial X_j} + \rho_0 f_i \qquad (13)$$

$$\dot{P}_{ij} = J\frac{\partial X_j}{\partial x_m}\left(C^{mat}_{imkl} + \sigma_{lm}\delta_{ik}\right)\frac{\partial \dot{u}_k}{\partial x_l} \qquad (14)$$

3.2 Arbitrariness Appearing in Solution of Equations in Deformation of Composite Materials

Equations (13) and (14) are unified to one differential equation.

$$\rho_0\frac{\partial^2 \dot{u}_i}{\partial t^2} - \rho_0\dot{f}_i = \frac{\partial}{\partial X_j}\left(A_{ijkl}\frac{\partial \dot{u}_k}{\partial x_l}\right) \qquad (15)$$

where tensor A_{ijkl} is

$$A_{ijkl} = J\frac{\partial X_j}{\partial x_m}\left(C^{mat}_{imkl} + \sigma_{lm}\delta_{ik}\right) \qquad (16)$$

Equation (15) plays a role of governing equation in the deformation of composite materials. When the reference configuration is taken at the moment of the present time, and in the place where the external force doesn't act, (15) becomes as follows,

$$\rho\frac{\partial^2 \dot{u}_i}{\partial t^2} = \frac{\partial}{\partial x_j}\left(A_{ijkl}\frac{\partial \dot{u}_k}{\partial x_l}\right) \qquad (17)$$

Here, we conduct the transformation of coordinate system for this equation. Firstly each variable is transformed as the following in the transformation of coordinate system.

$$dx_i = \frac{\partial x_i}{\partial x'_a}dx'_a,\ \ \dot{u}_i = \frac{\partial x_i}{\partial x'_a}\dot{u}'_a,\ \ \frac{\partial}{\partial x_l} = \frac{\partial x'_d}{\partial x_l}\frac{\partial}{\partial x'_d}$$

$$L_{kl} = \frac{\partial x_k}{\partial x'_c}\frac{\partial x'_d}{\partial x_l}\frac{\partial u'_c}{\partial x'_d} = \frac{\partial x_k}{\partial x'_c}\frac{\partial x'_d}{\partial x_l}L'_{cd},\ \ \sigma_{ij} = \frac{\partial x_i}{\partial x'_a}\frac{\partial x_j}{\partial x'_b}\sigma'_{ab}$$

$$A_{ijkl} = \frac{\partial x_i}{\partial x'_a}\frac{\partial x_j}{\partial x'_b}\frac{\partial x'_c}{\partial x_k}\frac{\partial x_l}{\partial x'_d}A'_{abcd} \qquad (18)$$

where x'_a is the coordinate system after the transformation. Then (17) is transformed as follows,

$$\rho\frac{\partial^2 \dot{u}'_a}{\partial t^2} = \frac{\partial}{\partial x'_b}\left(A'_{abcd}\frac{\partial \dot{u}'_c}{\partial x'_d}\right) \qquad (19)$$

Commonly the governing equations for natural phenomena do not change their form in the coordinate transformation. Next, when the deformation is locally isotropic in 2′ and 3′ direction, $\partial/\partial x'_2$ and $\partial/\partial x'_3$ are equal to zero, and when the deformation is quasi-static, $\partial/\partial t$ becomes equal to zero, which corresponds with the case when inertia term is infinitesimal, then Eq. (19) becomes as follows,

$$\frac{\partial}{\partial x'_1}\left(A'_{a1c1}\frac{\partial \dot{u}'_c}{\partial x'_1}\right) = 0 \qquad (20)$$

Here, the eigenvalue problem of the tensor A'_{a1c1} is considered. Using the eigenvalue λ' and the eigenvector v'_c of the tensor A'_{a1c1}, the eigenvalue problem is represented as

$$A'_{a1c1}v'_c = \lambda' v'_c \qquad (21)$$

When the tensor A'_{a1c1} has zero eigenvalues, (21) becomes as follows,

$$A'_{a1c1}v'_c = 0 \qquad (22)$$

Multiplying the arbitrary function $\phi'(x'_1)$,

$$A'_{a1c1}v'_c\phi'(x'_1) = 0 \qquad (23)$$

Taking the partial differenciation of x'_1,

$$A'_{a1c1}v'_c\frac{\partial}{\partial x'_1}\phi'(x'_1) = 0 \qquad (24)$$

This equation means that $\dot{u}'_c = v'_c\phi'(x'_1)$ is one of the solution of (20). Since $\dot{u}'_c = v'_c\phi'(x'_1)$ is the solution of (20) for arbitrary function $\phi'(x'_1)$, (20) have multiple solutions, or the arbitrariness appears in the solution of (20). This case causes when the tensor A'_{a1c1} has zero eigenvalues. When the tensor A'_{a1c1} has zero eigenvalues, the determinant of A'_{a1c1} becomes zero,

$$\det\left(A'_{a1c1}\right) = 0 \qquad (25)$$

From (18), the tensor A'_{a1c1} is represented by the original coordinate system of tensor A_{ijkl}.

$$A'_{a1c1} = A_{ijkl}\frac{\partial x'_a}{\partial x_i}\frac{\partial x'_1}{\partial x_j}\frac{\partial x_k}{\partial x'_c}\frac{\partial x'_1}{\partial x_l} \qquad (26)$$

Here, we introduce two tensors n_j and J_{ai} which express the coordinate transformation.

$$n_j = \frac{\partial x'_1}{\partial x_j},\ \ J_{ai} = \frac{\partial x'_a}{\partial x_i} \qquad (27)$$

Then (25) becomes as follows,

$$\det\left(A'_{a1c1}\right) = \det\left(A_{ijkl}n_j n_l J_{ai}J_{ck}^{-1}\right)$$
$$= \det\left(A_{ijkl}n_j n_l\right)\cdot\det\left(J_{ai}\right)\cdot\det\left(J_{ck}^{-1}\right) = 0 \qquad (28)$$

Since $\det\left(J_{ai}\right) \neq 0$,

$$\det\left(A_{ijkl}n_j n_l\right) = 0 \qquad (29)$$

As the conclusion of this analysis, when (29) is satisfied, the arbitrariness appears in the solution of (20) which is a specific case of the governing equations for the deformation of composite materials. Equation (29) is considered as the initiation condition of arbitrariness in the solution of the equations for the deformation of composite materials. This is interesting because in structural mechanics it is well recognized that the buckling of the structures is represented by a condition where the determinant of the stiffness matrix of the structures is equal to zero.

$$\det[K] = 0 \qquad (30)$$

where $[K]$ is the stiffness matrix. There is a significant similarity in between (29) and (30). In the case of (30), at the time when the equation has equality, the structural instability or the buckling phenomena appear in the structures, and the material and geometrical nonlinearity of the stiffness matrix play important roles in these instability or the buckling. In the case of (29), when the equation has equality, the material instability or the microbuckling phenomena appear in the materials, and the material nonlinearity including the effect of matrix nonlinear stress-strain relation and geometrical nonlinearity including the effect of fiber misalignment play important roles in these instability or the microbuckling. In addition, from (16), (29) also becomes as follows,

$$\det\left(C^{mat}_{ijkl} n_j n_l + \sigma_{jl}\delta_{ik} n_j n_l\right) = 0 \tag{31}$$

The first term of this equation depends on the constitutive tensor of the material, including the elastic and plastic property of the material. It is also related with the material nonlinear effect. The second term of the equation depends on the multi-axial stresses. It is related with the geometrical nonlinear effect. The equation indicates that the appearance of arbitrariness is related with the material property and the multi-axial stresses. The angle of microbuckling is able to affect through the variable n_j, but the width of the band of the microbuckling possibly does not affect the arbitrariness condition. It is also notable that due to the nonlinearity including the material and geometrical nonlinearity, the arbitrariness is able to appear, it indicates that the fact that the governing equations for the deformation of composite materials are nonlinear equations is essential for the appearance of arbitrariness. Considering the actual deformation, the resultant displacement in the arbitrariness seems to have the following formula,

$$\dot{u}'_c = v'_c H_L\left(x'_1 - c\right) \tag{32}$$

where the function $H_L\left(x'_1\right)$ is the Heaviside function. Since theoretically arbitrary displacement is allowed, the width of the band of microbuckling is able to relate with the initial misalignment shape in the material around the area of initiation of the microbucling. When we put the tensor $A_{ijkl} n_j n_l$ as a_{ik}, the determinant of (29) is explicitly represented in two-dimensional as the following,

$$\det a_{ik} = a_{11}a_{22} - a_{12}a_{21} = 0 \tag{33}$$

In fiber reinforced composite materials, commonly the elastic modulus in fiber axial direction has much higher value than the value of transverse direction and stress value, and because of this, C^{mat}_{1111} has much higher value than the other components of constitutive tensor C^{mat}_{ijkl} and the components of stress tensor σ_{ij}, that is $C^{mat}_{1111} >> C^{mat}_{ijkl}, \sigma_{ij}$ $\left(C^{mat}_{ijkl} \neq C^{mat}_{1111}\right)$. Since only A_{1111} and a_{11} includes C^{mat}_{1111}, $A_{1111} >> A_{ijkl}$ $\left(A_{ijkl} \neq A_{1111}\right)$ and $a_{11} >> a_{ik}$ $\left(a_{ik} \neq a_{11}\right)$. Thus the equation becomes,

$$a_{22} = \frac{a_{12}a_{21}}{a_{11}} \approx 0 \tag{34}$$

Here the vector n_j is represented using an angle β as follows,

$$n_j = \frac{\partial x'_1}{\partial x_j} = \left(\cos\beta \quad \sin\beta\right) \tag{35}$$

Then a_{22} is represented as follows,

$$\begin{aligned} a_{22} &= A_{2j2l} n_j n_l \\ &= C^{mat}_{2j2l} n_j n_l + \sigma_{jl} n_j n_l \\ &= \left(C^{mat}_{2121} + \sigma_{11}\right)\cos^2\beta + \left(C^{mat}_{2122} + C^{mat}_{2221} + 2\sigma_{12}\right) \\ &\qquad \cdot \cos\beta\sin\beta + \left(C^{mat}_{2222} + \sigma_{22}\right)\sin^2\beta \approx 0 \end{aligned} \tag{36}$$

From this equation,

$$\begin{aligned} -\sigma_{11} \approx C^{mat}_{2121} &+ \left(C^{mat}_{2222} + \sigma_{22}\right)\tan^2\beta \\ &+ \left(C^{mat}_{2122} + C^{mat}_{2221} + 2\sigma_{12}\right)\tan\beta \end{aligned} \tag{37}$$

$-\sigma_{11}$ is the value of applied compressive stress to the material in longitudinal direction. When this applied stress reaches the value of right hand side of (37), the determinant of (29) becomes equal to zero, and the arbitrariness is allowed to appear, which means the instability appears in the material and microbuckling is able to occur in the actual situations. The value of $-\sigma_{11}$ at the time of being equal to right hand side of (37) is considered as the critical compressive stress σ_{cr} or the buckling stress in microbuckling.

$$\begin{aligned} \sigma_{cr} \approx C^{mat}_{2121} &+ \left(C^{mat}_{2222} + \sigma_{22}\right)\tan^2\beta \\ &+ \left(C^{mat}_{2122} + C^{mat}_{2221} + 2\sigma_{12}\right)\tan\beta \end{aligned} \tag{38}$$

Using elastic-plastic tangent shear modulus G^{ep}_{LT}, transverse tangent modulus E^{ep}_T, in-plane Poisson's ratio ν_{12} and ν_{21} and shear stress τ_{12}, the equation becomes as follows,

$$\begin{aligned} \sigma_{cr} \approx G^{ep}_{LT} &+ \left(\frac{1}{1-\nu_{12}\nu_{21}}E^{ep}_T + \sigma_{22}\right)\tan^2\beta \\ &+ \left(C^{mat}_{2122} + C^{mat}_{2221} + 2\tau_{12}\right)\tan\beta \end{aligned} \tag{39}$$

In the case of uniaxial compression and if C^{mat}_{2122} and C^{mat}_{2221} are close to zero, the compressive strength is approximately represented as follows,

$$\sigma_{cr} \approx G^{ep}_{LT} + \frac{1}{1-\nu_{12}\nu_{21}}E^{ep}_T \tan^2\beta \tag{40}$$

Equation (40) corresponds with the expression given by Budiansky [8]. It is indicated that the arbitrariness condition in equations of deformation of composite materials is closely related with the initiation condition of compressive failure of composite materials.

3.3 Numerical Analysis for Fiber Microbuckling Stress Using Arbitrariness Condition

Here the numerical analysis is conducted for the actual material property using the arbitrariness condition. For this purpose, incremental analysis is conducted. As the initial condition, stress is set to zero. Then the stress is incrementally applied. In each increment, total stress is calculated and matrix plastic state is updated. Constitutive tensors of fiber, matrix, and composites are calculated, and the determinant in (29) is evaluated. When the determinant in (29) becomes approximately equal to zero, the arbitrariness is assumed to occur, and the microbuckling is assumed to initiate. At this increment, the calculation is finished, and the applied compressive stress at this time is recorded as the material strength or the microbuckling stress. For transverse failure modes, failure criteria presented by Pinho et al. [9] are applied. The material property of CFRP AS4/3501-6 [5] is assumed. For strain hardening curve of matrix, two kinds of hardening curves M and N shown in Fig. 2 are applied and the results are compared. The analysis is repeated with changing each one parameter, and the results for the relationship between material strength and each one parameter are obtained.

Fig. 5(a) shows the analysis results for the relationship between compressive strength and the multi-axial stresses. The shear stress reduces the compressive strength and this relation

ISSN 2229-5518

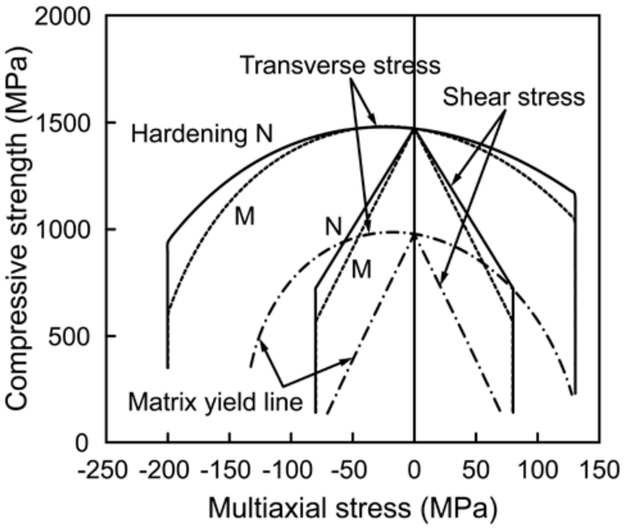

(a) Relationship with multi-axial stress

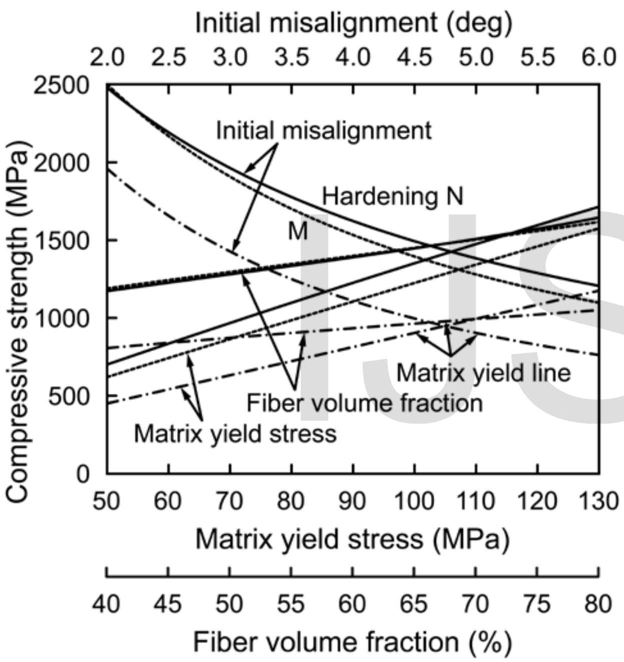

(b) Relationship with material property

Figure 5: Numerical results of compressive strength of the material.

is approximately represented as the linear relation. Tensile and high compressive transverse stress also reduces the compressive strength, while under the small compressive transverse stress, the compressive strength is almost constant. In addition, the dependency of the multi-axial stresses changes with the change of the strain hardening curve. Fig. 5(b) shows the analysis results for the relationship between compressive strength and the constituent material property. The matrix yield stress and fiber volume fraction increases the compressive strength and these relations are also close to the linear relation. The initial fiber misalignment reduces the compressive strength and this relation is close to the inversely proportional relation. The dependency of the material strength for each parameter almost agrees with the experimental results shown in the previous investigations [3].

4 Conclusion

A model of fiber microbuckling in composite materials is investigated. There exists a state where the arbitrariness appears in the solution of equations expressing the deformation of composite materials, and the condition for onset of the arbitrariness is closely related with the initiation of the fiber microbuckling and the material strength.

References

[1] J. LLorca, C. González, J. M. Molina-Aldareguía, J. Segurado, R. Seltzer, F. Sket, M. Rodríguez, S. Sádaba, R. Muñoz, and L. P. Canal, "Multiscale Modeling of Composite Materials: a Roadmap Towards Virtual Testing," *Advanced Materials*, vol. 23, no. 44, pp. 5130-5147, 2011.

[2] M. J. Hinton and P. D. Soden, "Predicting Failure in Composite Laminates: The Background to The Exercise," *Composites Science and Technology*, vol. 58, no. 7, pp. 1001-1010, 1998.

[3] C. R. Schultheisz and A. M. Waas, "Compressive Failure of Composites, Part I: Testing and Micromechanical Theories," *Progress in Aerospace Sciences*, vol. 32, no. 1, pp. 1-42, 1996.

[4] S. Basu, A. M. Waas, and D. R. Ambur, "Compressive Failure of Fiber Composites Under Multi-axial Loading," *Journal of the Mechanics and Physics of Solids*, vol. 54, no. 3, pp. 611-634, 2006.

[5] P. D. Soden, M. J. Hinton, and A. S. Kaddour, "Lamina Properties, Lay-up Configurations and Loading Conditions for a Range of Fibre-Reinforced Composite Laminates," *Composites Science and Technology*, vol. 58, no. 7, pp. 1011-1022, 1998.

[6] C. S. Yerramalli and A. M. Waas, "A failure criterion for fiber reinforced polymer composites under combined compression–torsion loading," *International Journal of Solids and Structures*, vol. 40, no. 5, pp. 1139–1164, 2003.

[7] K. Tohgo, Y. Sugiyama and K. Kawahara, "Ply-Cracking Damage and Nonlinear Deformation of CFRP Cross-Ply Laminate," *JSME International Journal*, *Series A*, vol. 45, no. 4, pp. 545-552, 2002.

[8] B. Budiansky, "Micromechanics," *Computers & Structures*, vol. 16, no. 1-4, pp. 3-12, 1983.

[9] S. T. Pinho, C. G. Davila, P. P. Camanho, L. Iannucci and P. Robinson, "Failure Models and Criteria for FRP under In-plane or Three-dimensional Stress States Including Shear Non-linearity," *TM-2005-213530*, 2005.